JOURNAL OF THEORETICAL AND APPLIED MECHANICS
51, 3, pp. 639-648, Warsaw 2013

THE COMPREHENSIVE FINITE ELEMENT MODEL FOR STENTING: THE INFLUENCE OF STENT DESIGN ON THE OUTCOME AFTER CORONARY STENT PLACEMENT

Misagh Imani, Ali M. Goudarzi, Davood D. Ganji, Amir L. Aghili
Department of Mechanical Engineering, Babol University of Technology, Babol, Iran
e-mail: misagh.imani@gmail.com; ddg_davood@yahoo.com

Stenting is one of the most important methods to treat atherosclerosis. Due to its simplicity and efficiency, the use of coronary stents in interventional procedures has rapidly increased, and different stent designs have been introduced in the market. In order to select the most appropriate stent design, it is necessary to analyze and compare the mechanical behavior of different types of stents. In this paper, the finite element method is used for analyzing the behavior of stents. The aim of this work is to investigate the expansion characteristics of a stent as it is deployed and implanted in an artery containing a plaque and propose a model as close to real conditions of stent implantation as possible. Furthermore, two commercially available stents (the Palmaz-Schatz and Multi-Link stents) are modeled and their behavior during the deployment is compared in terms of stress distribution, radial gain, outer diameter changes and dogboning. Moreover, the effect of stent design on the restenosis rate is investigated by comparing the stress distribution in the arteries. The results show the importance of considering the plaque in finite element simulation of mechanical behavior of the coronary stent. According to the findings, the possibility of restenosis is nonsignificantly lower for the Multi-Link stent in comparison with the Palmaz-Schatz stent, which is in good agreement with clinical results.

Key words: numerical model, coronary stent, balloon, plaque, vessel, FEM

1. Introduction

Nowadays, one of the most prevalent health problems is coronary heart disease. Coronary artery disease is specific to the arteries of the heart. Coronary artery disease, also known as atherosclerosis, occurs when fatty material, known as plaque, collects along the walls of arteries. Plaque is an intimal lesion that typically consists of an accumulation of cells, lipids, calcium, collagen, and inflammatory infiltrates and can thicken, harden and even block the arteries. Artery occlusion can significantly reduce the blood flow through the artery and leads to serious problems, such as heart attack, stroke, or even death.

Several procedures are available to revascularise an occluded artery, including balloon angioplasty and stenting, bypass surgery and atherectomy (Pericevic *et al.*, 2009). A stent is a tubular scaffold which can be inserted into a diseased artery to relieve the narrowing caused by a stenosis. Since stent implantation, namely stenting, does not require any surgical operation and has less complication, pain and a more rapid recovery compared to the other possible treatments, the use of coronary stents in interventional procedures has rapidly increased in recent years. Only in the United States, 1.2 million patients undergo stent implantations each year (Gu *et al.*, 2010).

A successful stent implantation is dependent on the good understanding of its behavior during its deployment. There are two methods to analyze the behavior of the stent: experimental methods and numerical simulations. In comparison with expensive experiments carried out in hospitals and laboratories, numerical simulations accomplished by computers have advantages

in both flexibility and cost. For this reason, the use of numerical methods in analyzing the performance of the coronary stent has increased. In recent publications, different numerical models, with different level of complexity and accuracy, have been proposed to simulate the expansion during deployment of the coronary stent. In the early works, single stent models were used without considering the contact effect (Chua *et al.*, 2002; Dumoulin and Cochelin, 2000; Gu *et al.*, 2005; McGarry *et al.*, 2004; Migliavacca *et al.*, 2002). Later on, in order to obtain better results, more complicated models have been proposed, such as the balloon-stent model (Chua *et al.*, 2003, 2004a; Ju *et al.*, 2008; Xia *et al.*, 2007; Wang *et al.*, 2006), stent-artery model with plaque (Lally *et al.*, 2005), balloon-stent-artery model without plaque (Walke *et al.*, 2005) and balloon-stent-artery model with plaque (Wu *et al.*, 2007; Chua *et al.*, 2004b). Furthermore, different formulations of constitutive models for artery and plaque have been proposed in the literature, including linear isotropic (Walke *et al.*, 2005; Chua *et al.*, 2004b) or hyperelastic material models (Pericevic *et al.*, 2009; Lally *et al.*, 2005; Wu *et al.*, 2007). Moreover, extensive studies were found in the literature that did not consider the blood flow (Pericevic *et al.*, 2009; Chua *et al.*, 2002, 2004b; Wu *et al.*, 2007), although Lally *et al.* (2005) and Gervaso *et al.* (2008) tried to simulate the blood pressure by applying a constant internal pressure to the artery and plaque.

With attention to the mentioned background, it is necessary to propose a model as close to real conditions of stent implantation as possible. The first aim of this paper is to present a more accurate model that contains internal blood pressure, balloon, stent, plaque and vessel. Moreover, a bi-linear elasto-plastic model was chosen for the stent material while the balloon, artery and plaque were simulated using a hyperelastic material model.

On the other hand, because of wide acceptance of coronary stenting, a rapidly increasing number of different stent types with different materials and designs has been introduced in the market. In order to select the most appropriate stent type, it is necessary to analyze and compare the behavior of different types before utilizing. One of the most important issues that must be considered during the comparison process is in-stent restenosis (ISR). In-stent restenosis is a re-narrowing or blockage of an artery at the same site where stenting has already taken place. As reported in Gu *et al.* (2010), the restenosis rate correlates with the stress concentration in the stented vessel wall. Because of the influence of the stent design on the stress field within the artery wall, the stent design is one of the most important factors that may affect the process of restenosis after stent implantation (Kastrati *et al.*, 2000). Furthermore, stent design influences the dogbone effect of stent implantation (De Beule *et al.*, 2006). Therefore, stent design has a significant impact on the outcome after coronary stent placement. Despite this, most of the works regarding the effect of stent design on its behavior are clinical (Kastrati *et al.*, 2000; Baim *et al.*, 2001; Lansky *et al.*, 2001; Kobayashi *et al.*, 1999; Miketic *et al.*, 2001) and few numerical works have been performed in this respect (Lally *et al.*, 2005; Balossino *et al.*, 2008). So that, the second aim of this paper is to compare the mechanical behavior of different stent types by means of numerical models based on the finite element method. Two commercially available stents, with the same material and different designs, were studied and the behavior of the models was compared in terms of stress distribution, radial gain, outer diameter changes and dogboning. Furthermore, the effect of stent design on the restenosis rate was investigated by comparing the stress distribution in the arteries.

2. Materials and methods

Two models were developed, each constituted by the same balloon and coronary artery with plaque, and a different stent design. Modeling of various parts used in simulating is presented in this section. Commercially available software has been used.

2.1. Stent

Two different coronary stent designs were taken into consideration. They resemble two commercial intravascular stents: Palmaz-Schatz (Johnson & Johnson Interventional System, Warren, NJ, USA) and Multi-Link RX Ultra^{TM} coronary stent (Guidant-Advanced Cardiovascular Systems, Inc., Santa Clara, CA, USA). In the following, they will be referred to as STENT A and STENT B for Palmaz-Schatz and Multi-Link, respectively.

The STENT A is a first generation stent, but the STENT B represents a novel second generation coronary stent and incorporates the presence of two different types of elements:

(i) tubular-like rings and

(ii) bridging members (links).

The first one functions to maintain the vessel open after the stent expansion and the second one to link the rings in a flexible way during the delivery process. Hence, the tubular-like rings determine the stiffness whilst the bridging members determine the flexibility of the overall structure.

The primary model of stents was produced using commercially available software. Models were constructed on the basis of images from the literature (Serruys and Kutryk, 2000). The main geometrical dimensions of the simulated models are assumed to be the same. Both stents have an outer diameter of 3 mm, a length of 10 mm, and a thickness of 0.05 mm. Figure 1 shows the two-stent models in their unexpanded configuration.

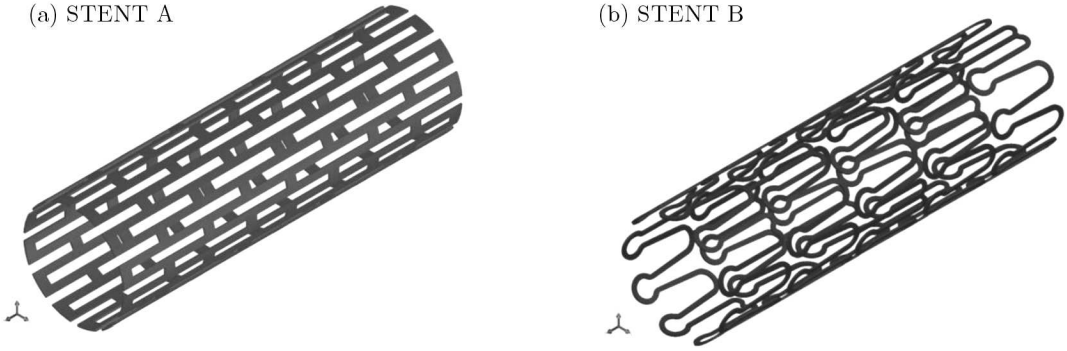

Fig. 1. Geometry of two-stent models in their unexpanded configuration (a) STENT A, (b) STENT B

The stents were assumed to be made of stainless steel 304. A bi-linear elasto-plastic material model was used to model the behavior of the stents material. The material properties were chosen same as those assumed in Chua *et al.* (2003), which are as: Young's modulus = 193 GPa; shear modulus = $75 \cdot 10^6$ MPa; tangent modulus = 692 MPa; density = $7.86 \cdot 10^{-6}$kg/mm^3; yield strength = 207 MPa; Poisson's ratio = 0.27.

2.2. Artery with plaque

With the assumption of a homogenous and isotropic material, the coronary artery was modeled as an idealized vessel. The geometrical properties of the vessel and plaque are: vessel length = 20 mm; inner diameter = 4 mm; outer diameter = 5 mm; plaque length = 3 mm; plaque inner diameter = 3 mm.

The vessel and plaque were modeled as a hyperelastic material with the Mooney-Rivlin (M-R) description. Using the hyperelastic model of an incompressible isotropically elastic solid, the Cauchy stress σ_{ij}, may be given in terms of the left Cauchy-Green tensor B_{ij} as (Green and Zerna, 1968)

$$\sigma_{ij} = -p + 2\frac{\partial W}{\partial I_1}B_{ij} - 2\frac{\partial W}{\partial I_2}B_{ij}^{-1} \tag{2.1}$$

where W is the strain-energy density function, while I_1, I_2 and I_3 are the invariants of B_{ij} which can be defined in terms of the principal stretches of the material λ_1, λ_2 and λ_3 as

$$I_1 = \lambda_1^2 + \lambda_2^2 + \lambda_3^2 \qquad I_2 = \lambda_1^2\lambda_2^2 + \lambda_1^2\lambda_3^2 + \lambda_2^2\lambda_3^2 \qquad I_3 = \lambda_1^2\lambda_2^2\lambda_3^2 \tag{2.2}$$

The general polynomial form of the strain-energy density function for the isotropic hyperelastic material can be written as (Carew *et al.*, 1968)

$$W(I_1, I_2, I_3) = \sum_{i,j,k=0}^{\infty} C_{ijk}(I_1 - 3)^i(I_2 - 3)^j(I_3 - 3)^k \qquad C_{000} = 0 \tag{2.3}$$

where C_{ijk} are the material coefficients determined from the experiments. Incompressible nature of vascular tissue was established by Carew *et al.* (1968). For the incompressible material, the third invariant is given as $I_3 = 1$. The specific hyperelastic constitutive model used to model the arterial tissue in this study is a specific form of Eq. $(2.3)_1$, whereby the strain-energy density function is a third-order hyperelastic model suitable for an incompressible isotropic material and has the form given as

$$W = C_{10}(I_1 - 3) + C_{01}(I_2 - 3) + C_{20}(I_1 - 3)^2 + C_{11}(I_1 - 3)(I_2 - 3) + C_{30}(I_1 - 3)^3 \tag{2.4}$$

This M-R form of the constitutive equation is included in several finite element codes and is therefore readily applicable to stent design. Substituting Eq. (2.4) into Eq. (2.1), the stress components can be easily obtained. Table 1 summarizes the coefficients used for the hyperelastic constitutive equations of the two material models (Lally *et al.*, 2005).

Table 1. Hyperelastic coefficients to describe the arterial tissue and stenotic plaque non-linear elastic behavior

	Arterial wall tissue [kPa]	Stenotic plaque tissue [kPa]
C_{10}	18.90	−495.96
C_{01}	2.75	506.61
C_{20}	85.72	1193.53
C_{11}	590.43	3637.80
C_{30}	0	4737.25

2.3. Balloon

The balloon as a medium to expand the stent was modeled to be 12 mm in length. The outer diameter and the thickness of the balloon were 2.9 mm and 0.1 mm, respectively. A polyurethane rubber type material was used to represent the balloon. Polyurethane is an incompressible material and was defined by a nonlinear first-order hyperelastic M-R model, in which the strain--energy density function was given as

$$W = C_{01}(I_1 - 3) + C_{10}(I_2 - 3) \tag{2.5}$$

The energy function coefficients used are: $C_{01} = 0.710918$ MPa, $C_{10} = 1.06881$ MPa. The material density is equal to $1070\,\mathrm{kg/m^3}$ (Chua *et al.*, 2003; Xia *et al.*, 2007).

2.4. Meshing and boundary conditions

Due to the symmetrical conditions, only a quarter of the STENT A and one-third of the STENT B were used to simulate the expansion process. For both models, all parts were meshed

with eight-node linear 3D block elements. Sensitivity analyses were performed to ensure enough meshing refinement. Models A and B include 13288 and 26140 elements, respectively. Moreover, an automatic surface to the surface algorithm approach available in software was selected in order to cope with the nonlinear contact problem among the surfaces. Figure 2 shows the assembled model for STENT A.

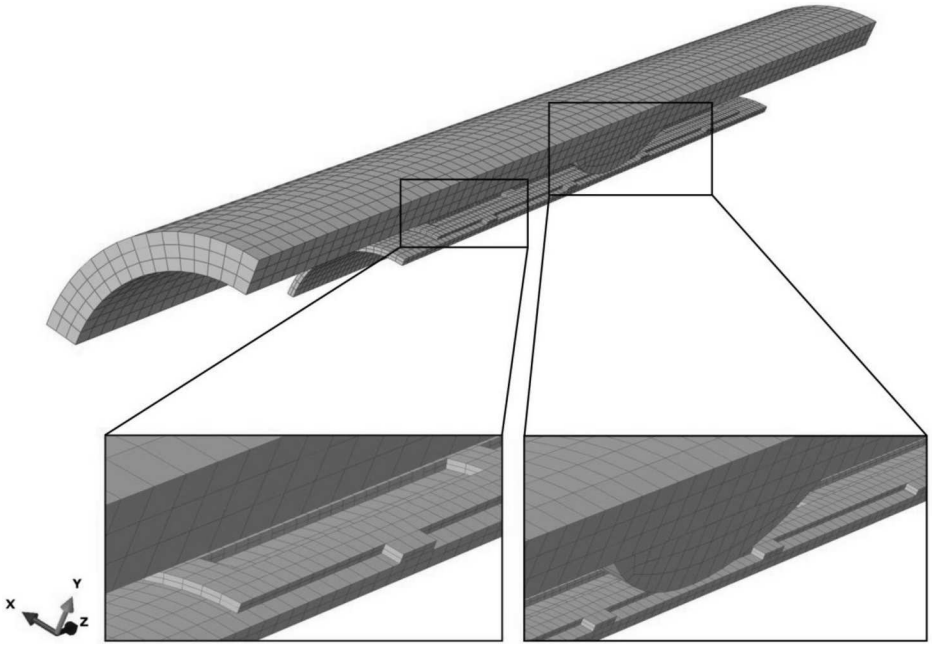

Fig. 2. The assembled model for STENT A

Symmetric constraints were imposed to corresponding symmetry nodes of the balloon, stent, vessel and plaque. Both ends of the balloon were considered to be fully fixed. Furthermore, only the movement in the radial direction was permitted for the nodes located at the two ends of the vessel, and the plaque was attached to the vessel.

2.5. Loading and solutions

The loading process of both models consisted of two steps. In the first step, without considering the existence of the balloon and the stent, a constant internal pressure equal to 13.3 kPa was applied to the vessel and the plaque. This pressure was equal to the blood pressure of 100 mmHgs (Lally *et al.*, 2005). The pressure simulates the internal pressure of the blood and causes the vessel to expand, and also, induces an initial stress. This step causes the modeled vessel and the plaque to be as close to the reality as possible. In the second step, by keeping the initial pressure applied to the vessel and plaque, a constant pressure was imposed to the internal surface of the balloon. This pressure was applied with a constant rate in 1.635 seconds and its value was varied from 0 to 0.41 MPa for STENT A and 0 to 0.3 MPa for STENT B.

3. Results and discussion

In this section, the results of the finite element analysis of the expansion of stents inside an atherosclerotic coronary artery are presented. The results include stress distribution, radial gain and outer diameter changes, dogboning and restenosis rate. These results could deserve consideration when designing stents.

3.1. Stress distribution

The distribution of von Mises stress in the two-stent models is shown in Fig. 3 at the maximum expansion instant. As can be seen in Fig. 3a, in STENT A, the regions of high stress are located at the four corners of the cells. This is because of the struts being pulled apart from each other to form a rhomboid shape of cells during the expansion. The value of maximum von Mises stress in the stent is 257.5 MPa, which is in good agreement with Chua *et al.* (2003), which shows the maximum von Mises stress of 249 MPa in the same stent model without considering the vessel and plaque. As expected, in the current model, longitudinal and circumferential symmetries are observed in the stress distribution, which validates the modeling and imposed boundary conditions. The regions of high stress in STENT B (Fig. 3b) are located at the curvature of the tubular-like rings, and the value of maximum von Mises stress is 254.7 MPa. Furthermore, it is possible to observe the effect of considering the plaque on the deformed configurations reached by the two-stent models.

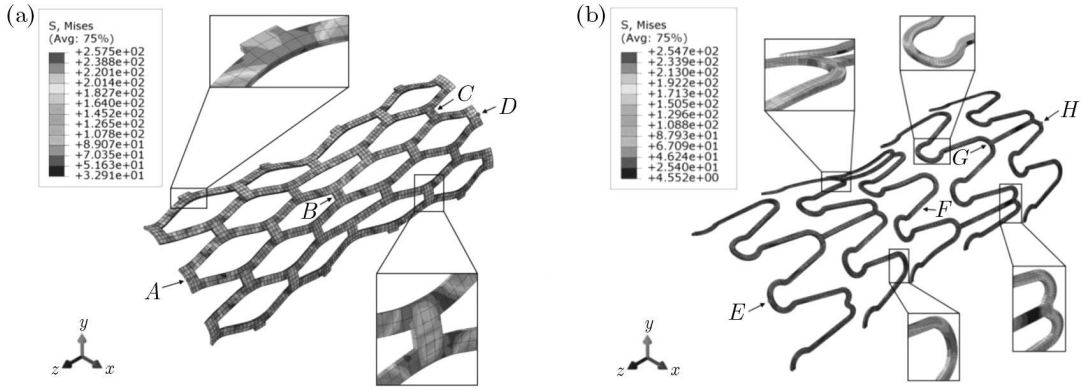

Fig. 3. Distribution of von Mises stress in (a) STENT A; (b) STENT B

Von Mises stress in the expanded vessels is depicted in Fig. 4 for the two geometries investigated. The highest arterial stresses are in the areas where the maximum changes occurred in stents diameter. The value of maximum von Mises stress in the vessel is 0.282 MPa and 0.244 MPa, for STENT A and B, respectively. Possible damage to the artery might occur at these critical points. Furthermore, because of the presence of the plaque, the stress distribution in the vessel is different from the study by Walke *et al.* (2005). This shows the importance of considering the plaque in finite element simulation of mechanical behavior of the coronary stent. Moreover, the von Mises stresses show a considerable gradient from the internal to the external surface of the arterial wall.

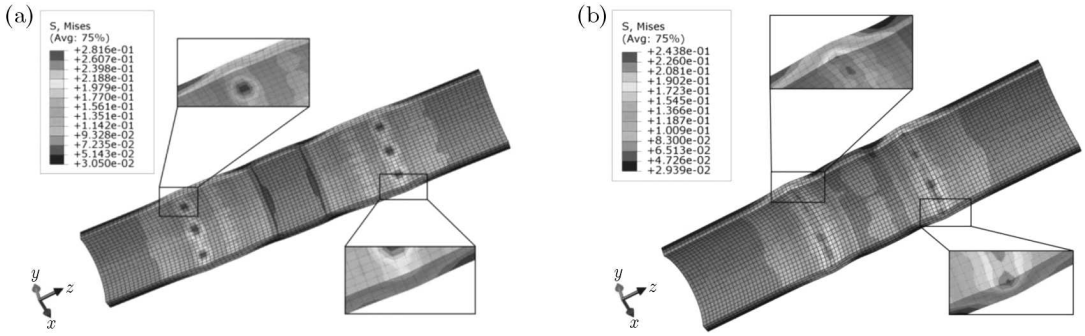

Fig. 4. Distribution of von Mises stress in the expanded vessel at the maximum expansion (a) STENT A; (b) STENT B

3.2. Radial gain and outer diameter changes

The radial gain (RG) is one of the most important parameters to evaluate the performance of the stent, which is defined as follow

$$RG = R_{expansion} - R_0 \tag{3.1}$$

where $R_{expansion}$ and R_0 are the outer radius of the stent, after and before the expansion, respectively. RG is measured at the middle of the stent. Note that the value of RG represents the final radial deformation, and a greater value of RG is more appropriate in practical applications. The value of RG is 0.357 mm and 0.363 mm for STENT A and B, respectively. It means that their final diameters are approximately equal.

For a better understanding of the expansion behavior of the two-stent models, Fig. 5 plots the outer diameter of stents against the expanding pressure. As can be seen in Fig. 3, because of the existence of the plaque and the pressure applied by it, different positions of stents have different diameters. Here, in order to verify the behavior of two models, the outer diameter changes of points B, C in STENT A, and F, G in STENT B (as shown in Fig. 3) were derived and shown.

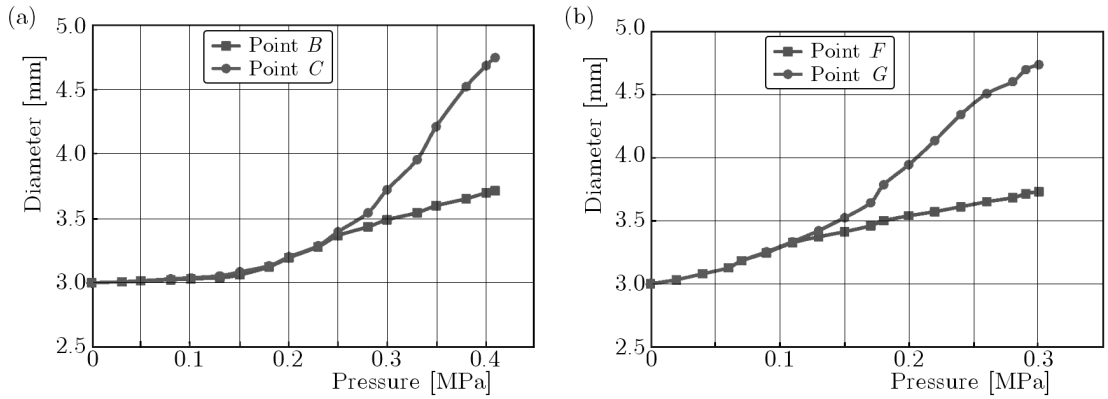

Fig. 5. The relation between the outer diameter of the stent and expanding pressure for (a) STENT A; (b) STENT B

Figure 5a shows that the rate of increment of the stent diameter at points B and C is almost identical as pressure changes from 0 MPa to 0.25 MPa. From the pressure 0.25 to 0.33 MPa, because of the contact between point B and the plaque, the stent diameter increases with a low rate at point B, while at point C, the rate of increment of the diameter grows significantly. Finally, for pressures larger than 0.33 MPa, because of the contact between the stent and the vessel, the variation of diameter at point C becomes small. The same behavior was observed for STENT B (Fig. 5b) although its critical points are different (the critical points are 0.11 MPa and 0.28 MPa, respectively).

3.3. Dogboning

When the stent expands, because of different distribution of the circumferential stress between the free ends and the central part, it bends on edges that causes the diameter at the end sides becomes larger than that of the middle of the stent. This phenomenon is called "dogboning". The dogboning of the stent will change as its geometric design alters. According to the findings of the clinical studies, a stent is expected to have low dogboning (Mario and Karvouni, 2000; Carrozza *et al.*, 1999). The dogboning is defined as

$$\begin{aligned} \text{dogboning}_{distal} &= \frac{R_{distal} - R_{central}}{R_{central}} \qquad distal = left, right \\ \text{dogboning} &= \sum_{distal} \left|\text{dogboning}_{distal}\right| \qquad distal = left, right \end{aligned} \tag{3.2}$$

where subscripts $(distal = left, right)$ indicate where the deformed structure is measured. Points A and D for STENT A, and points E and H for STENT B are *left* and *right*, respectively.

Figure 6 plots the relation between the dogboning and the expanding pressure. As shown in this figure, for STENT A, in pressures of 0.25 MPa and 0.33 MPa, the rate of dogboning is changed because of contact of the stent to the plaque and vessel whilst these alterations happen in pressures of 0.11 MPa and 0.28 MPa for STENT B. Furthermore, STENT A had the final dogboning value of 0.6, which is more than for STENT B (0.47). This shows the better performance of STENT B in comparison with STENT A.

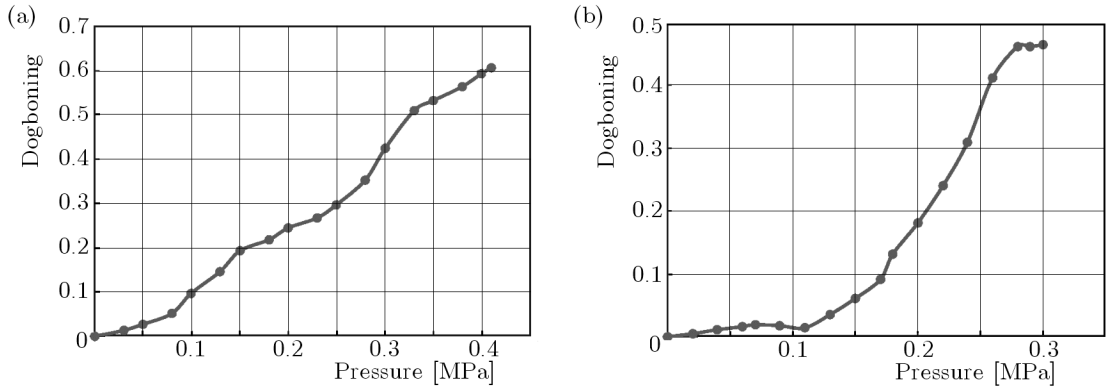

Fig. 6. The relation between dogboning and expanding pressure for (a) STENT A; (b) STENT B

3.4. Restenosis rate

In-stent restenosis (ISR) still remains an obsession to cardiologists (Wu *et al.*, 2007). It has recently been shown that stress concentration in the stented vessel wall correlates with the restenosis rate (Gu *et al.*, 2010), and the possibility of ISR increases by increasing the stress in the vessel wall. Changes of stent cell geometry may affect the stress field within the artery wall and consequently influence the restenosis rate.

Numerous clinical trials have looked into the influence of stent design on outcome after coronary stent placement (Kastrati *et al.*, 2000; Baim *et al.*, 2001; Kobayashi *et al.*, 1999; Miketic *et al.*, 2001; Kastrati *et al.*, 2001). These works can confirm the results obtained in this study. The findings of the current paper indicate that the possibility of restenosis in STENT A is a little more than STENT B, due to the nonsignificantly higher value of maximum arterial stresses in STENT A. Furthermore, because of the sharp curvature at the ends (as demonstrated in Fig. 3) and a large value of dogboning, STENT A causes more injury in the vessel than STENT B. This agrees with the results obtained in Baim *et al.* (2001), Kastrati *et al.* (2001). Results like those obtained in this study can be used to compare the possibility of restenosis of different stent designs.

4. Conclusion

The paper presents a methodology for modeling the expansion of coronary stents used in the treatment of blood vessel stenosis. In order to achieve a more realistic description of the stent implantation procedure, the model includes internal pressure of blood, balloon, stent, vessel and plaque. Two commercially available stent models were analyzed and compared in this study.

According to the analysis, in Palmaz-Schatz stent, the possibility of failure at the four corners of the cells is more than at the other places, as these are the regions with maximum stresses, whilst in Multi-Link stent, the critical points are located at the curvature of the tubular-like rings. Even when both stents expanded to the same final diameters, the maximum stress induced in the artery by the Palmaz-Schatz stent was obtained 15.57% more than by the Multi-Link stent. Furthermore, the dogboning value of Palmaz-Schatz stent is 30.43% higher than the other one. Consequently, it is predictable that using the Palmaz-Schatz stent results in more injury in the vessel than the Multi-Link stent, which increases the possibility of restenosis. These results agree with the clinical studies which confirm that the possibility of restenosis was nonsignificantly lower for Multi-Link stent in comparison with Palmaz-Schatz stent (Baim *et al.*, 2001).

As mentioned in Baim *et al.* (2001), the regulatory agencies such as the U.S. Food and Drug Administration require that a new stent prove to be equivalent to an approved stent. This sets the stage for a series of "stent versus stent" randomized trials designed to show that each newer stent design was not inferior to (i.e., equivalent or better than) the prior approved stent. The numerical model presented in this study, when joined with these clinical trials, could be used as a beneficial tool to investigate the influence of the stent design on the outcome after coronary stent placement.

References

1. Baim D.S., Cutlip D.E., Midei M., Linnemeier T.J., Schreiber T., Cox D., et al., 2001, Final results of a randomized trial comparing the MULTI-LINK stent with the Palmaz-Schatz stent for narrowings in native coronary arteries, *American Journal of Cardiology*, **87**, 157-162
2. Balossino R., Gervaso F., Migliavacca F., Dubini G., 2008, Effects of different stent designs on local hemodynamics in stented arteries, *Journal of Biomechanics*, **41**, 1053-1061
3. Carew T.E., Vaishnav R.N., Patel D.J., 1968, Compressibility of the arterial wall, *Circulation Research*, **22**, 61-68
4. Carrozza J.P., Susanne E.H., David J.C., 1999, In vivo assessment of stent expansion and recoil in normal porcine coronary arteries, *Circulation*, **100**, 756-760
5. Chua S.N.D., MacDonald B.J., Hashmi M.S.J., 2002, Finite-element simulation of stent expansion, *Journal of Materials Processing Technology*, **120**, 335-340
6. Chua S.N.D., MacDonald B.J., Hashmi M.S.J., 2003, Finite element simulation of stent and balloon interaction, *Journal of Materials Processing Technology*, **143/144**, 591-597
7. Chua S.N.D., MacDonald B.J., Hashmi M.S.J., 2004a, Effects of varying slotted tube (stent) geometry on its expansion behaviour using finite element method, *Journal of Materials Processing Technology*, **155/156**, 1764-1771
8. Chua S.N.D., MacDonald B.J., Hashmi M.S.J., 2004b, Finite element simulation of slotted tube (stent) with the presence of plaque and artery by balloon expansion, *Journal of Materials Processing Technology*, **155/156**, 1772-1779
9. De Beule M., Van Impe R., Verhegghe B., Segers P., Verdonck P., 2006, Finite element analysis and stent design: Reduction of dogboning, *Technology and Health Care*, **14**, 233-241
10. Dumoulin C., Cochelin B., 2000, Mechanical behaviour modelling of balloon-expandable stents, *Journal of Biomechanics*, **33**, 1461-1470
11. Gervaso F., Capelli C., Petrini L., Lattanzio S., Di Virgilio L., Migliavacca F., 2008, On the effects of different strategies in modelling balloon-expandable stenting by means of finite element method, *Journal of Biomechanics*, **41**, 1206-1212
12. Green A.E., Zerna W., 1968, *Theoretical Elasticity*, Clarendon Press, Oxford
13. Gu L., Santra S., Mericle R.A., Kumar A.V., 2005, Finite element analysis of covered microstents, *Journal of Biomechanics*, **38**, 1221-1227

14. Gu L., Zhao S., Muttyam A.K., Hammel J.M., 2010, The relation between the arterial stress and restenosis rate after coronary stenting, *Journal of Medical Devices*, **4**, 031005

15. Ju F., Xia Z., Sasaki K., 2008, On the finite element modelling of balloon-expandable stents, *Journal of the Mechanical Behavior of Biomedical Materials*, **1**, 86-95

16. Kastrati A., Dirschinger J., Boekstegers P., Elezi S., Schuhlen H., Pache J., et al., 2000, Influence of stent design on 1-year outcome after coronary stent placement: A randomized comparison of five stent types in 1147 unselected patients, *Catheterization and Cardiovascular Interventions*, **50**, 290-297

17. Kastrati A., Mehilli J., Dirschinger J., Pache J., Ulm K., Schuhlen H., et al., 2001, Restenosis after coronary placement of various stent types, *American Journal of Cardiology*, **87**, 34-39

18. Kobayashi Y., De Gregorio J., Kobayashi N., Reimers B., Albiero R., Vaghetti M., et al., 1999, Comparison of immediate and follow-up results of the short and long NIR stent with the Palmaz-Schatz stent, *American Journal of Cardiology*, **84**, 499-504

19. Lally C., Dolan F., Prendergast P.J., 2005, Cardiovascular stent design and vessel stresses: a finite element analysis, *Journal of Biomechanics*, **38**, 1574-1581

20. Lansky A.J., Roubin G.S., O'Shaughnessy C.D., Moore P.B., Dean L.S., Raizner A.E., et al., 2000, Randomized comparison of GR-II stent and Palmaz-Schatz stent for elective treatment of coronary stenoses, *Circulation*, **102**, 1364-1368

21. Marion C.D., Karvouni E., 2000, The bigger, the better: true also for in-stent restenosis? *European Heart Journal*, **21**, 710-711

22. Maurel W., Wu Y., Magnenat N., Thalmann D., 1998, *Biomechanical Models for Soft-Tissue Simulation*, Springer, Berlin

23. McGarry J.P., O'Donnell B.P., McHugh P.E., McGarry J.G., 2004, Analysis of the mechanical performance of a cardiovascular stent design based on micromechanical modelling, *Computational Materials Science*, **31**, 421-438

24. Migliavacca F., Petrini L., Colombo M., Auricchio F., Pietrabissa R., 2002, Mechanical behavior of coronary stents investigated through the finite element method, *Journal of Biomechanics*, **35**, 803-811

25. Miketic S., Carlsson J., Tebbe U., 2001, Randomized comparison of J&J Crown stent versus NIR stent after routine coronary angioplasty, *American Heart Journal*, **142**, E8

26. Pericevic I., Lally C., Toner D., Kelly D.J., 2009, The influence of plaque composition on underlying arterial wall stress during stent expansion: The case of lesion-specific stents, *Medical Engineering and Physics*, **31**, 428-433

27. Serruys P.W., Kutryk M.J.B., 2000, *Handbook of Coronary Stents*, 3rd ed., Martin Dunitz Ltd., London

28. Walke W., Paszenda Z., Filipiak J., 2005, Experimental and numerical biomechanical analysis of vascular stent, *Journal of Materials Processing Technology*, **164/165**, 1263-1268

29. Wang W.Q., Liang D.K., Yang D.Z., Qi M., 2006, Analysis of the transient expansion behavior and design optimization of coronary stents by finite element method, *Journal of Biomechanics*, **39**, 21-32

30. Wu W., Wang W.Q., Yang D.Z., Qi M., 2007, Stent expansion in curved vessel and their interactions: A finite element analysis, *Journal of Biomechanics*, **40**, 2580-2585

31. Xia Z., Ju F., Sasaki K., 2007, A general finite element analysis method for balloon expandable stents based on repeated unit cell (RUC) model, *Finite Elements in Analysis and Design*, **43**, 649-658

Manuscript received June 28, 2012; accepted for print November 14, 2012